AD-A161 186 OSCILLATING FLOW ABOUT CIRCULAR CYLINDERS AT LOW KEULEGAN-CARPENTER NUMBERS(U) NAVAL POSTGRADUATE SCHOOL MONTEREY CA N Q YUEN SEP 85 1/1

UNCLASSIFIED F/G 20/4 NL

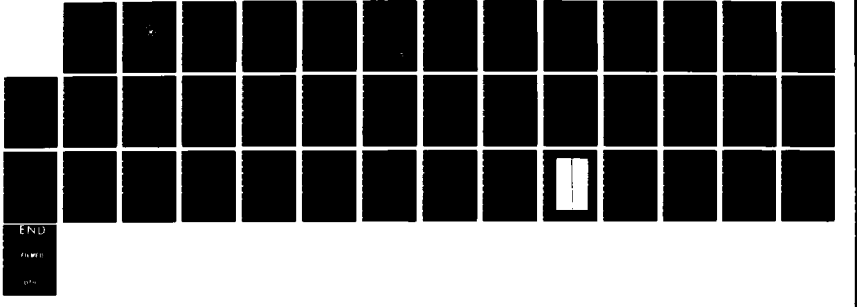

END

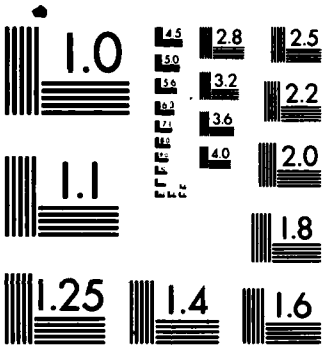

MICROCOPY RESOLUTION TEST CHART
NATIONAL BUREAU OF STANDARDS-1963-A

NAVAL POSTGRADUATE SCHOOL
Monterey, California

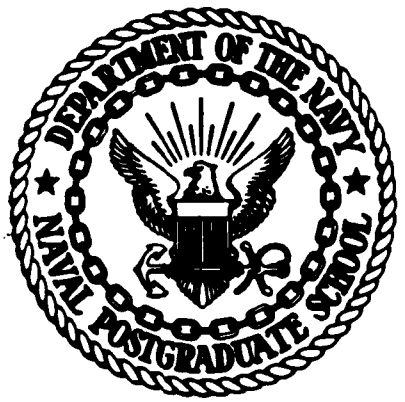

THESIS

OSCILLATING FLOW ABOUT CIRCULAR CYLINDERS AT LOW KEULEGAN-CARPENTER NUMBERS

by

Nathan Q.S. Yuen

September 1985

Thesis Advisor: T. Sarpkaya

Approved for public release; distribution is unlimited

SECURITY CLASSIFICATION OF THIS PAGE (When Data Entered)

REPORT DOCUMENTATION PAGE

READ INSTRUCTIONS BEFORE COMPLETING FORM

1. REPORT NUMBER	2. GOVT ACCESSION NO. AD-A161186
3. RECIPIENT'S CATALOG NUMBER	
4. TITLE (and Subtitle) Oscillating Flow About Circular Cylinders at Low Keulegan-Carpenter Numbers	5. TYPE OF REPORT & PERIOD COVERED Master's Thesis; September 1985
	6. PERFORMING ORG. REPORT NUMBER
7. AUTHOR(s) Nathan Q. S. Yuen	8. CONTRACT OR GRANT NUMBER(s)
9. PERFORMING ORGANIZATION NAME AND ADDRESS Naval Postgraduate School Monterey, California 93943-5100	10. PROGRAM ELEMENT, PROJECT, TASK AREA & WORK UNIT NUMBERS
11. CONTROLLING OFFICE NAME AND ADDRESS Naval Postgraduate School Monterey, California 93943-5100	12. REPORT DATE September 1985
	13. NUMBER OF PAGES 39
14. MONITORING AGENCY NAME & ADDRESS(if different from Controlling Office)	15. SECURITY CLASS. (of this report) Unclassified
	15a. DECLASSIFICATION/ DOWNGRADING SCHEDULE

16. DISTRIBUTION STATEMENT (of this Report)

Approved for public release; distribution is unlimited

17. DISTRIBUTION STATEMENT (of the abstract entered in Block 20, if different from Report)

18. SUPPLEMENTARY NOTES

19. KEY WORDS (Continue on reverse side if necessary and identify by block number)

Oscillating Flow; Inertia-Dominated Regime; Drag and Inertia Coefficients; Flow at Low Keulegan-Carpenter Numbers; Wave Forces; Pipelines.

20. ABSTRACT (Continue on reverse side if necessary and identify by block number)

The in-line force and the resulting drag and inertia coefficients for smooth and rough circular cylinders immersed in a sinusoidally oscillating flow at low Keulegan-Carpenter numbers (K) have been determined experimentally and compared with those obtained theoretically by Stokes and Wang. In addition, flow visualization experiments were carried out with oscillating cylinders in a water table and the stability

DD FORM 1 JAN 73 1473 EDITION OF 1 NOV 65 IS OBSOLETE

S N 0102-LF-014-6601

SECURITY CLASSIFICATION OF THIS PAGE (When Data Entered)

20. (Continued)

of the flow was investigated. The results have shown that for very low values of K, the flow about the cylinder is laminar, attached, and stable and the drag coefficient is nearly identical to that predicted theoretically. At a critical K, the flow becomes unstable to Taylor-Görtler vortices and the drag coefficient jumps to a higher value. Subsequently, the flow separates, becomes turbulent and results in a minimum drag coefficient. The subsequent increases in drag are attributed to vortex shedding. The inertia coefficient agrees with that obtained theoretically in the range where the flow is laminar.

ABSTRACT

The in-line force and the resulting drag and inertia coefficients for smooth and rough circular cylinders immersed in a sinusoidally oscillating flow at low Keulegan-Carpenter numbers (K) have been determined experimentally and compared with those obtained theoretically by Stokes and Wang. In addition, flow visualization experiments were carried out with oscillating cylinders in a water table and the stability of the flow was investigated. The results have shown that for very low values of K, the flow about the cylinder is laminar, attached, and stable and the drag coefficient is nearly identical to that predicted theoretically. At a critical K, the flow becomes unstable to Taylor-Görtler vortices and the drag coefficient jumps to a higher value. Subsequently, the flow separates, becomes turbulent and results in a minimum drag coefficient. The subsequent increases in drag are attributed to vortex shedding. The inertia coefficient agrees with that obtained theoretically in the range where the flow in laminar.

Approved for public release; distribution is unlimited

Oscillating Flow About Circular Cylinders at Low Keulegan-Carpenter Numbers

by

Nathan Q.S. Yuen
Lieutenant, United States Navy
B.S., University of Hawaii, 1977

Submitted in partial fulfillment of the requirements for the degree of

MASTER OF SCIENCE IN MECHANICAL ENGINEERING

and the degree of

MECHANICAL ENGINEER

from the

NAVAL POSTGRADUATE SCHOOL
September 1985

Author: Nathan Q. S. Yuen

Approved by: Turgut Sarpkaya, Thesis Advisor

Paul J. Marto, Chairman, Department of Mechanical Engineering

John N. Dyer, Dean of Science and Engineering

TABLE OF CONTENTS

LIST OF FIGURES

TABLE OF SYMBOLS AND ABBREVIATIONS

A	Amplitude of flow oscillation
a_n	Fourier coefficient
C_a	Added mass coefficient
C_d	Drag coefficient
$C_f(rms)$	RMS value of calculated force
C_m	Inertia coefficient
D	Cylinder diameter
F	In-line force
F_m	Measured in-line force
K	Keulegan-Carpenter number, $K = U_m T/D = 2\pi A/D$
K_{cr}	Critical Keulegan-Carpenter number
k	Mean sand-roughness height
k/D	Relative roughness
L	Cylinder length
p	Pressure
Re	Reynolds number, $Re = U_m D/\nu$
T	Period of flow oscillation
t	Time
U	Instantaneous velocity
U_m	Maximum velocity in a cycle
u	x-component of velocity
v	y-component of velocity

x	Horizontal component of coordinate axis
y	Vertical component of coordinate axis
β	Frequency parameter, $\beta = Re/K = D^2/\nu T$
θ	Angle, $\theta = 2\pi t/T$
ν	Kinematic viscosity of water
ρ	Density of water
ω	Circular frequency

ACKNOWLEDGEMENT

I wish to thank Distinguished Professor Turgut Sarpkaya for the privilege of working with him on this research project. Through his example, I have developed the basic skills and the desire for further personal and professional growth.

My appreciation is extended to Mr. Jack McKay who transformed designs into working models.

I. INTRODUCTION

The determination of the forces acting on bluff bodies immersed in time dependent flows has been of special interest in many branches of engineering. Special attention has been devoted to the wave forces on offshore structures. The extensive laboratory and field studies of the past decade have yielded extremely interesting results regarding the in-line and transverse forces acting on smooth and rough cylinders [Ref. 1]. However useful these investigations were, they were based on the use of an empirical equation (Morison's) [Ref. 2] and on the force coefficients obtained either through the Fourier Analysis or the method of least squares. In recent years, it became quite clear that further progress toward the understanding of the physics of the phenomenon must be based on analytical studies and the understanding of the kinematics of the flow.

A theoretical analysis of the separated flow about a circular cylinder is an extremely difficult problem. Efforts in that direction through the use of the discrete vortex models did not lead to meaningful conclusions. It became clear that the key towards the understanding of flow separation, transition and vortex formation is in the very low Keulegan-Carpenter number (K) regime. It is because of

this reason that experiments were carried out in an oscillating water tunnel for force measurements and with an oscillating cylinder in a water table for flow visualization. The investigation resulted in findings beyond the original objectives. In the following, first the theoretical analysis and then the experimental apparatus and measurements will be presented. These will be followed by a discussion of the results and conclusions.

II. ANALYSIS

A. INTRODUCTION

This section will present a condensed review of the theoretical studies regarding the oscillating flow about bluff bodies. First the flow about an infinite flat plate undergoing sinusoidal oscillations will be briefly discussed. Then Schlichting's [Refs. 3 and 4], Stokes' [Ref. 5 and 6], and finally Wang's [Ref. 7] solution of a sinusoidally oscillating cylinder in a still fluid will be discussed. It should be emphasized that the case of a cylinder oscillating in a fluid otherwise at rest is identical to that of a fluid oscillating about a cylinder. The only difference comes from the 'buoyant' force acting on the cylinder in the direction of flow due to the pressure gradient needed to accelerate the flow, i.e., the inertia coefficient for the case of the oscillating flow is equal to $(1 + C_a)$ where C_a is the added mass coefficient for the oscillating cylinder, i.e., $C_m = 1 + C_a$.

B. STOKES' OSCILLATING PLATE PROBLEM

The flow about an infinite flat plate undergoing sinusoidal oscillations was treated by Stokes assuming that the flow is laminar and stable. With respect to the coordinate axis in Figure 1, the Navier-Stokes equations and the boundary conditions reduce to:

$$\frac{\partial u}{\partial t} = \nu \frac{\partial^2 u}{\partial y^2} \tag{1}$$

initial condition: $u(y,0) = 0$

boundary conditions: $u(0,t) = U_o \cos \omega t$

$u(\infty,t) = 0$

The solution of Eq. (1) via the separation of variables is given by:

$$u(y,t) = U_o \exp(-y\sqrt{\frac{\omega}{2\nu}}) \cos(\omega t - y\sqrt{\frac{\omega}{2\nu}}) \tag{2}$$

Letting $\eta = y\sqrt{\frac{\omega}{2\nu}}$, one has

$$u(y,t) = U_o \exp(-\eta) \cos(\omega t - \eta) \tag{3}$$

"The velocity profile u(y,t) has the form of a damped harmonic oscillation, the amplitude of which is $U_o \exp(-y\sqrt{\frac{\omega}{2\nu}})$ in which a fluid layer at a distance y has a phase lag with respect to the motion of the wall [Ref. 3]." Figure 2 shows the velocity distribution in the neighborhood of the oscillating wall.

C. SCHLICHTING'S OSCILLATING CYLINDER PROBLEM

Schlichting [Refs. 3 and 4] considered the case of a cylinder oscillating at high frequency and small amplitude

in a fluid otherwise at rest and used the boundary layer approximation to the Navier-Stokes equations. This led to:

$$\frac{\partial u}{\partial t} + u \frac{\partial u}{\partial x} + v \frac{\partial u}{\partial y} = - \frac{1}{\rho} \frac{\partial p}{\partial x} + \nu \frac{\partial^2 u}{\partial y^2} \tag{4}$$

which reduces to:

$$- \frac{1}{\rho} \frac{\partial p}{\partial x} = \frac{\partial U}{\partial t} + U \frac{\partial U}{\partial x} \tag{5}$$

for the outer flow, i.e., at the edge of the boundary layer. Combining Eqs. (4) and (5), one has:

$$\frac{\partial u_1}{\partial t} - \nu \frac{\partial^2 u_1}{\partial y^2} = \frac{\partial U}{\partial t} + U \frac{\partial U}{\partial x} \tag{6}$$

This equation may be solved to the desired degree of approximation. The first order (linear) approximation yields:

$$\frac{\partial u_1}{\partial t} - \nu \frac{\partial^2 u_1}{\partial y^2} = \frac{\partial U}{\partial t} \tag{7}$$

For the approximation to be valid, the convective acceleration must be considered smaller than the local acceleration, i.e.,

$$U \frac{\partial U}{\partial x} \ll \frac{\partial U}{\partial t} \tag{8}$$

Using the order of magnitude arguments, one has:

$$U \frac{\partial U}{\partial x} \sim \frac{U_m^2}{D}, \quad \frac{\partial U}{\partial t} = U_m \omega$$

It is seen that for the analysis to be valid, one must have $\frac{U_m T}{D} \ll 1$ or $\frac{A}{D} \ll 1$ where U_m is the maximum velocity in a cycle; T, the period of oscillation; D, the diameter of the cylinder; and A, the amplitude of oscillation.

The solution of Eq. (7) with the following boundary conditions:

at $y = 0$, $u = 0$ (no slip condition)

at $y = \infty$, $u = U$

yields the following stream function:

$$\psi_1(x,y,t) = \sqrt{\frac{\nu}{\omega}}\ U_o(x)\ f(\eta) e^{i\omega t} \tag{9}$$

from which one obtains the velocity as:

$$u(x,y,t) = U_o(x)[\cos(\omega t) - \exp(-\eta/\sqrt{2})\cos(\omega t - \eta/\sqrt{2})] \tag{10}$$

which is seen to be identical to Stokes' solution for the oscillating infinite flat plate.

A second approximation may be applied to Eq. (4) by retaining the convective terms. Then one has:

$$\frac{\partial u_2}{\partial t} - \nu \frac{\partial u^2_2}{\partial y^2} = U \frac{\partial U}{\partial x} - u_1 \frac{\partial u_1}{\partial x} - v_1 \frac{\partial u_1}{\partial y} \qquad (11)$$

The stream function needed for the solution of the above equation is given by:

$$\psi_2(x,y,t) = \sqrt{\frac{\nu}{\omega}}\, U_o(x) \frac{dU_o}{dx} \frac{1}{\omega} \{f_{2p}(\eta) e^{2i\omega t} + f_{2s}(\eta)\} \qquad (12)$$

where f_{2p} represents the periodic motion and f_{2s}, the steady state. The use of the following boundary conditions on f_{2p}:

$$\text{at } \eta = 0 \quad u == 0 \quad ==> \quad f = f' = 0$$
$$\text{at } \eta = \infty \quad f' = 0$$

and on f_{2s}:

$$\text{at } \eta = 0 \quad u = v = 0 \quad ==> \quad f = f' = 0$$
$$\text{at } \eta = \infty \quad f' = 0$$

leads to an important result. The boundary condition at $\eta = \infty$, $f' = 0$, for the steady state component cannot be met. Instead a finite value is obtained:

$$u_2(x,\infty) = -\frac{3}{4\omega} U_o \frac{dU_o}{dx} \tag{13}$$

Periodically oscillating flow about a circular cylinder produces a steady streaming motion outside the boundary layer. In Figure 3 the streamlines about an oscillating cylinder in a still fluid are shown. This is for the case for a small Reynolds number with K -> 0 which leads to four recirculation cells and four stagnatiton points around the cylinder.

The force acting on the cylinder has not been evaluated by Schlichting.

D. STOKES' OSCILLATING CYLINDER PROBLEM

Stokes, as one of his considerable achievements, investigated the flow about oscillating cylinders and spheres without resort to the boundary layer approximation [Refs. 5 and 6]. His solutions are then valid at an as yet unspecified small Reynolds number. His solution yields the following force per unit length of a cylinder:

$$\frac{F}{\frac{1}{2}\rho U_m^2 D} = \frac{4\pi^2}{K}\left(\frac{1}{\sqrt{\pi\beta}} + \frac{1}{\pi\beta}\right)\cos\omega t - \frac{\pi^2}{K}\left(1 + \frac{4}{\sqrt{\pi\beta}}\right)\sin\omega t \tag{14}$$

which can be obtained by use of the asymptotic expansion of the Bessel function for large values of β, ($\beta = D^2/\nu T$). Stokes' solution will be taken up again later following the discussion of a more recent solution.

E. WANG'S OSCILLATING CYLINDER PROBLEM

Wang [Ref. 7] in 1968, investigated the flow about an oscillating circular cylinder by taking into consideration the effects of curvature which were neglected in Schlichting's analysis. Using inner and outer expansion and the boundary layer approximation, Wang obtained the following force expression for the oscillating cylinder, valid to the order of $\beta^{-3/2}$:

$$\frac{F}{\frac{1}{2}\rho U_m^2 D} = \frac{4\pi^2}{K}\left(\frac{1}{\sqrt{\pi\beta}} + \frac{1}{\pi\beta} - \frac{1}{4\pi\beta\sqrt{\pi\beta}}\right)\cos\omega t - \frac{\pi^2}{K}\left(1 + \frac{4}{\sqrt{\pi\beta}} + \frac{1}{\pi\beta\sqrt{\pi\beta}}\right)\sin\omega t$$

$$+ \text{higher order terms} \qquad (15)$$

A comparison of Eqs. (14) and (15) shows that the first two terms in the corresponding parentheses are identical and Wang's solution differs from that of Stokes only in the third term. It is noted that both solutions are valid only for large β and thus they yield virtually identical results, since the third term in each parenthesis in Eq. (15) is negligible.

F. MORISON'S EQUATION AND THE STOKES AND WANG SOLUTIONS

The normalized form of the Morison equation, with $U = U_m \cos \omega t$, [Ref. 2] may be written as:

$$\frac{F}{\frac{1}{2}\rho U_m^2 D} = C_d \, |\cos \theta| \cos \theta - \frac{\pi^2}{K} C_m \sin \theta \qquad (16)$$

which was developed for the determination of wave forces on offshore structures and discussed in the literature in great detail during the past 30 years [Ref. 1].

The force expression obtained by Stokes and Wang may be expressed in the form of Morison's equation by linearizing $|\cos \theta| \cos \theta$.

From [Ref. 8], writing:

$$|\cos \theta| \cos \theta = \sum_{n=0}^{\infty} \frac{\int_0^{2\pi} |\cos \theta| \cos \theta \cos n\theta \, d\theta}{\int_0^{2\pi} \cos^2 n\theta \, d\theta} \qquad (17)$$

$$= a_o + a_1 \cos \theta + a_2 \cos 2\theta + \ldots$$

with: $a_n = 0$ n even

$$a_n = (-1)^{\frac{n+1}{2}} \frac{8}{n(n^2 - 4)\pi} \quad \text{n odd}$$

$$a_1 = \frac{8}{3\pi}$$

using a first term approximation:

$$|\cos\ \theta|\ \cos\ \theta = \frac{8}{3\pi}\cos\ \theta \tag{18}$$

Then Eq. (15) may be reduced to:

$$C_m = 2 + 4\frac{1}{\sqrt{\pi\beta}} + \frac{1}{\pi\beta}\ \frac{1}{\sqrt{\pi\beta}} \tag{19}$$

$$C_d = \frac{3\pi^3}{2K}\left(\frac{1}{\sqrt{\pi\beta}} + \frac{1}{\pi\beta} - \frac{1}{4\pi\beta\sqrt{\pi\beta}}\right) \tag{20}$$

for the case of the <u>oscillating flow about a cylinder</u> (note: $C_m = 1 + C_a$). These drag and inertia coefficients will be compared with those obtained experimentally with smooth and rough cylinders.

III. EXPERIMENTAL EQUIPMENT AND PROCEDURES

Force measurements were carried out in a large U-shaped water tunnel. It is 34 feet long, 25 feet high, and has a working cross section of 3 feet by 4.66 feet. Additional details of the design and operation of the water tunnel are given in [Refs. 9 and 10]. The flow in the tunnel is oscillated by means of a 1 HP fan and a butterfly valve system. The frequency of oscillation of the butterfly valve is adjusted by means of an electronic feedback control system, so as to oscillate the flow at its natural frequency. The amplitude of oscillations can be maintained at the desired level by opening or closing a gate at the exit of the fan.

The test cylinders, approximately 3 feet in length, are mounted horizontally and supported at both ends by force transducers. These transducers can measure both the in-line and transverse forces. The electronic signals from the force transducers and from the amplitude gages are fed to two amplifiers and then digitized by means of an A/D converter. The digitized signal is then analyzed by means of a computer.

The experiments for each cylinder were repeated at least twice to ascertain the repeatability of the data.

Two smooth cylinders with $\beta = 1035$ and $\beta = 1380$ and one rough cylinder with $\beta = 1800$ were tested.

Flow visualization experiments were carried out in a 4 foot by 8 foot water table. Circular cylinders of suitable diameter were oscillated by means of a slider-crank mechanism and a variable speed motor. The flow pattern about the cylinder was made visible by means of an electro-chemical technique [Ref. 11]. For this purpose a solder wire was inbedded along the cylinder length. Voltage of 5 - 10 volts were applied between the solder and an electrode (placed away from the cylinder) to generate a metallic white smoke from the solder. A small amount of NaCl was added to the water to increase conductivity. Careful adjustment of the applied voltage and the repeated cleaning of the solder and cylinder surfaces were necessary for the successful visualization of the resulting flow patterns.

IV. PRESENTATION AND DISCUSSION OF RESULTS

The drag and inertia coefficients were evaluated through the use of Fourier averaging [Ref. 1], as given by:

$$C_d = -\frac{3}{4}\int_{\emptyset}^{2\pi} \frac{F_m \cos\theta}{\rho D U_m^2}\, d\theta$$

$$C_m = \frac{2K}{\pi^3}\int_{\emptyset}^{2\pi} \frac{F_m \sin\theta}{\rho D U_m^2}\, d\theta$$

Figures 4 and 5 show the drag and inertia coefficient, for a smooth cylinder, as a function of K for β = 1035 and β = 1380. Similar data are shown in Figure 6 for a rough cylinder (k/D = 1/100) for β = 1800. Also shown in Figures 4 through 6 is the drag coefficient obtained theoretically by Wang, Eq. (15).

Figures 4 and 5 show that C_d follows the theoretical line for a K value smaller than a critical K_{cr} and then increases almost abruptly to a higher value. Subsequently, C_d decreases with increasing K and reaches a minimum at a K value of about 2. The variation of C_d with K for K > 5 has been well documented in the literature [Ref. 3] and will not be dealt with here further.

Figure 5 is similar to Figure 4 in many respects with the addition of a hysteresis in the drag coefficient. For very small values of K, C_d followed the Wang-line and then rapidly jumped to a higher value. However, when the experiments were carried out by decreasing K at suitable intervals of K (with 15 minutes between each sampling), C_d remained at its higher value and then rapidly jumped back to the Wang-line at a K value smaller than that found in experiments with increasing K. The reason for the observed hysteresis is not easy to explain and it may be due to the precarious nature of the stability of the flow to the prevailing disturbances. It is tempting to think that in the experiments with decreasing K the level of the ambient turbulence is higher and this forces K_{cr} to occur at a lower K. In the future, it may be desirable to wait longer periods of time between two successive changes of K.

Figure 6 does not show any region where C_d agrees with Wang's prediction. In fact, from the lowest K obtainable in the present experiments to the K at which C_d goes through a minimum, Wang's prediction is considerably lower than that obtained experimentally. One will have to postulate that the flow has already become critical at K values smaller than about Ø.45 and one is observing only the post-critical region of the drag coefficient.

Figures 4 through 6 show that the inertia coefficient obtained experimentally agrees quite well with that given

by Wang for values of K smaller than K_{cr}. It is noted that both the theoretical and experimental values of C_m are slightly larger than 2 due to the effects of viscosity in the boundary layer. It should also be noted that there is very little or no scatter in the C_m data because the flow is in the inertia dominated regime.

Figure 7 shows the RMS (root mean square) value of the normalized in-line force as a function of K for all the cylinders tested. The theoretical value of the said coefficient is given by:

$$C_f(\text{rms}) = \sqrt{\frac{3}{8} C_d^2 + \frac{\pi^4 C_m^2}{2K^2}}$$

which is seen to agree well with the data for K smaller than about 8. This is due to the fact that the effect of C_d on $C_f(\text{rms})$ is quite small and the value of $C_f(\text{rms})$ is dictated by C_m.

The in-line force measurements and the resulting drag and inertia coefficients have revealed certain heretofore unknown facts which are both interesting and surprising. Interesting in the sense that the flow exhibits numerous transitions as K varies from about 0.4 to say 20. Surprising in the sense that one would not have expected transitions and hysteresis at relatively small K values

particularly prior to the separation of flow which was expected to occur at a K value in the vicinity of 1.0 - 2.0. These two observations led to the flow visualization studies noted earlier.

Figure 8 shows a sample photograph of the flow pattern about an oscillating cylinder. Clearly, Taylor-Görtler vortices form around the cylinder at regular intervals when the amplitude of oscillation exceeds a particular value. Figure 9 shows a plot of K versus β for smooth cylinders. For K values smaller than a critical K and for a given β the flow remains stable and attached. The symbol 'O' denotes the K value at which the Taylor-Görtler instability has manifested itself. This instability gradually leads to separation and turbulence as K is increased. The symbol 'X' denotes the K values at which the flow has become turbulent in the boundary layer beyond which no clear vortices were observable.

It is in light of Figure 9 that one can interpret the changes in C_d in Figures 4 through 6. For β = 1035 the instability starts at $K_{cr} \approx 1.05$, according to Figure 9. In Figure 4 the jump in C_d occurs at a slightly lower K. Nevertheless, it is now clear that the rapid changes in C_d in Figures 4 and 5 are a consequence of the instability observed in the flow. It is also seen that the K value at which the boundary layer becomes turbulent nearly

corresponds to the K value at which the drag coefficient goes through its minimum.

The foregoing discussion has not addressed itself to the case of rough cylinders. Exploratory experiments with a sand roughened oscillating cylinder have shown that the effect of roughness is to reduce K_{cr}. In fact, it was found that $K_{cr} \approx 0.4$ at $\beta = 1800$. Such a low K value was not attainabile in the force measurements with the rough cylinder due to a number of reasons, the most important being the noise level in the signal. Thus, it is safe to assume that the flow for the rough cylinder has become unstable at a K value at about 0.4 or less and led to the rapid increase in C_d prior to the lowest shown in Figure 6.

In summary, it is now clear from the measurements and observations that the theoretical predictions of Stokes and Wang agree with the measurements as long as the flow is lmainar, attached, and stable. As the flow becomes unstable to Taylor-Görtler vortices, the drag coefficient is drastically affected primarily due to changes in the shear stress level and distribution over the cylinder. The next important change in the flow and in the force coefficients takes place when the flow separates and the boundary layer becomes turbulent. The inception of separation nearly corresponds to the occurrence of minimum drag. Beyond that the pressure drag becomes increasingly dominant and the

shear becomes negligible as K increases. Contrary to the previous assumptions, that C_d varies from Ø to its maximum value as K varies from Ø - 12, it is seen that there are both interesting and important phenomena in the low Keulegan-Carpenter number regime. The experiments described here, however difficult they may have been due to the problems associated with the measurements of very small forces, have shed considerable light on the low K flow regime.

V. CONCLUSIONS

The investigation reported herein warranted the following conclusions:

1. The theoretical solutions of the oscillating flow about a circular cylinder are valid only for attached, stable, and laminar flow;

2. The flow becomes unstable to Taylor-Görtler vortices at a critical Keulegan-Carpenter number for a given ratio of the Reynolds number to the Keulegan-Carpenter number, i.e., β;

3. The drag coefficient shows a rapid jump at or near the critical Keulegan-Carpenter number. This is often accompanied by hysteresis;

4. There is a second critical Keulegan-Carpenter number at which the boundary layer separates and becomes turbulent. This paricular value of K nearly corresponds to the K value at which the minimum drag occurs;

5. The theoretical value of the inertia coefficient agrees with that determined experimentally only in the attached, laminar, and stable flow regime; and

6. Roughness precipitates transition and increases the drag coefficient. The effect of roughness on the inertia coefficient in the stable flow regime is negligible.

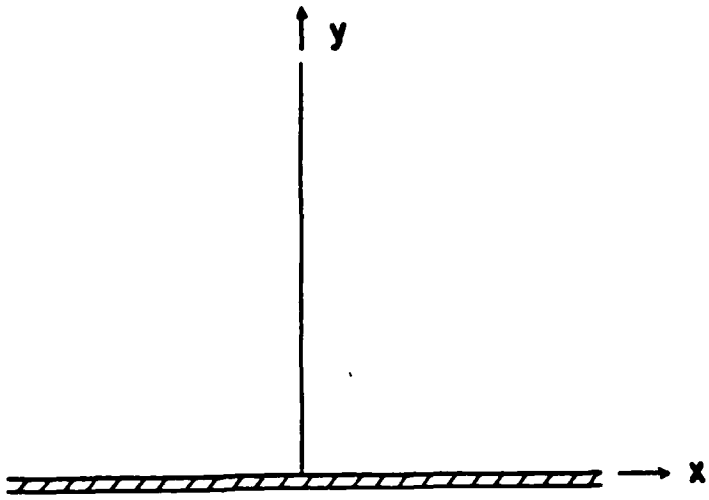

Figure 1. Coordinate Axis for an Oscillating Flat Plate

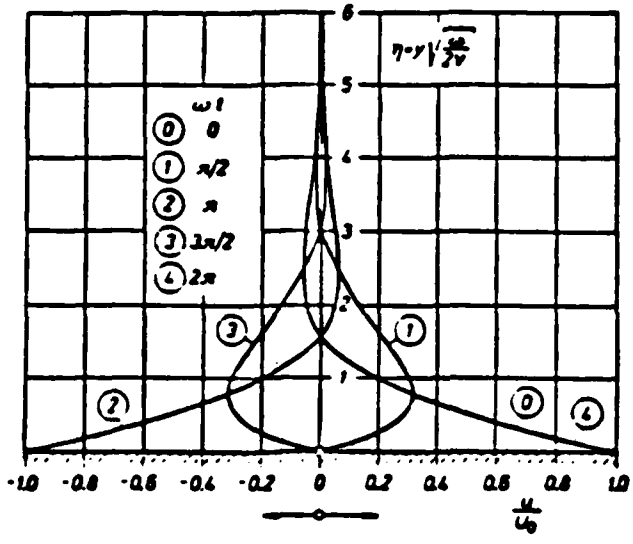

Figure 2. Velocity Distribution for Stokes' Oscillating Flat Plate

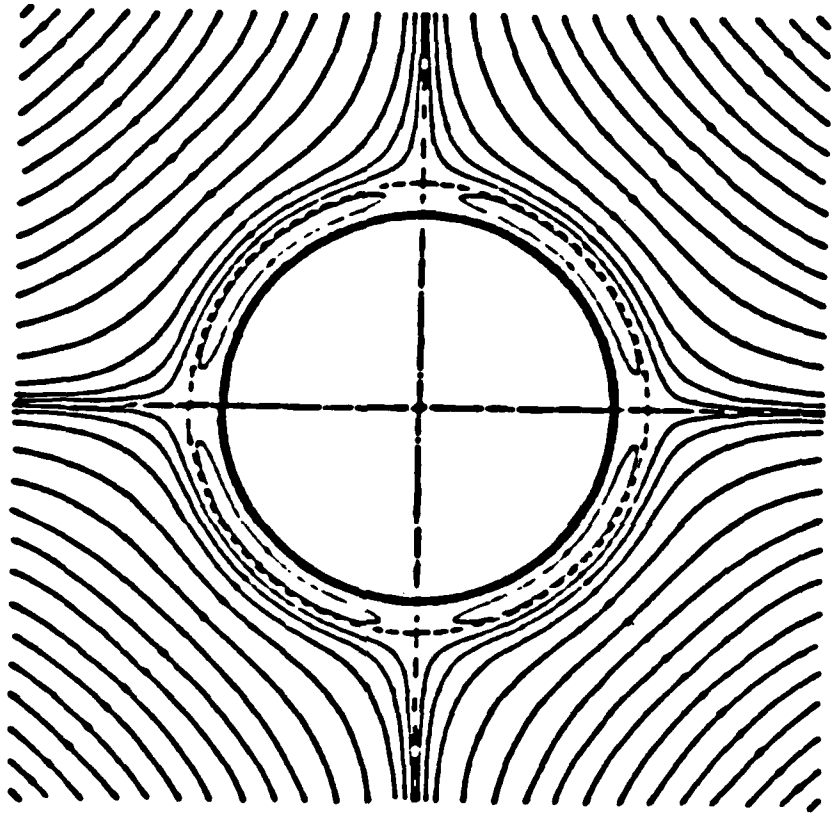

Figure 3. Streamline Pattern of Steady Motion of an Oscillating Circular Cylinder

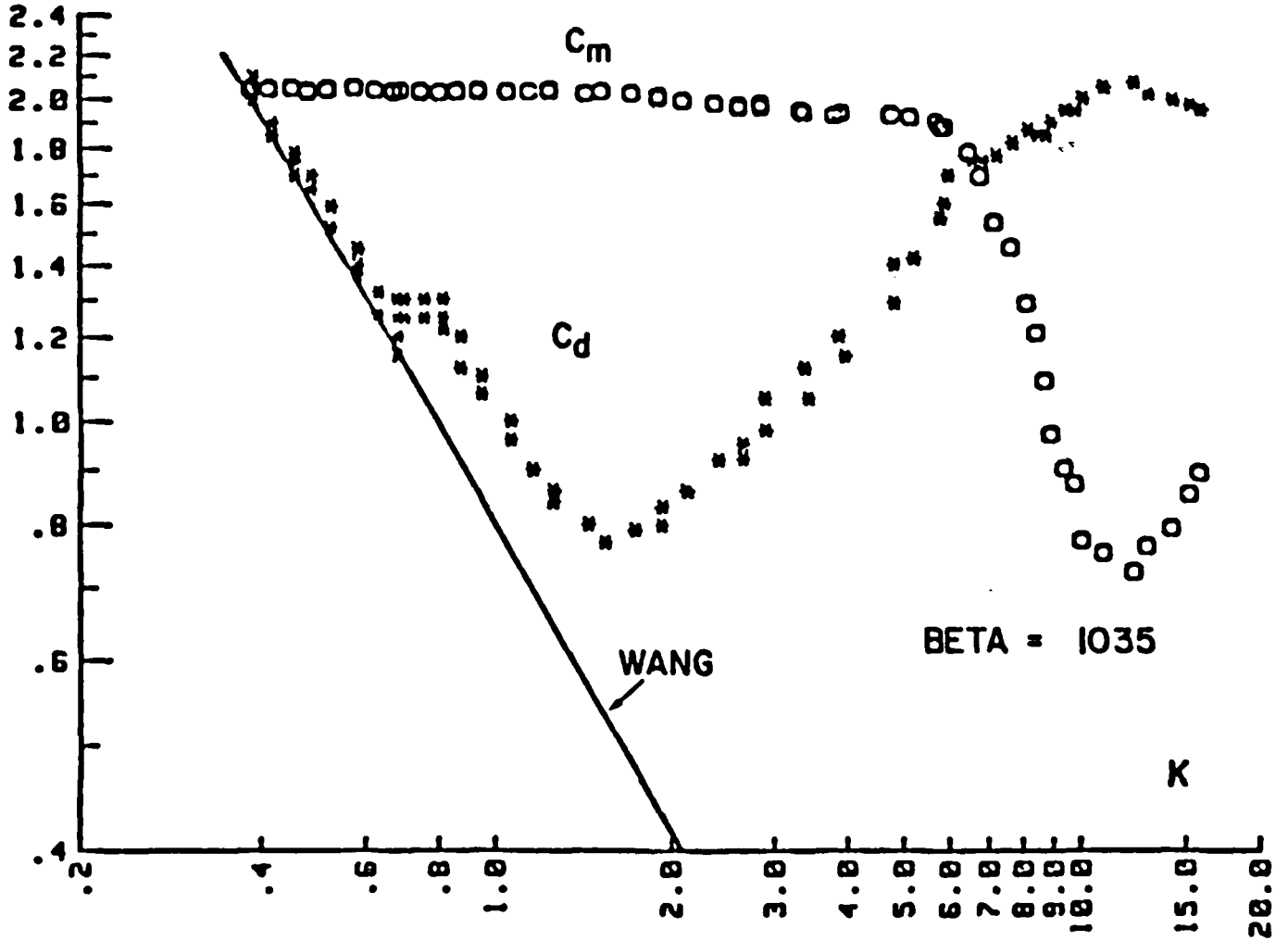

Figure 4. Drag and Inertia Coefficients versus K for β = 1035, Smooth Cylinder

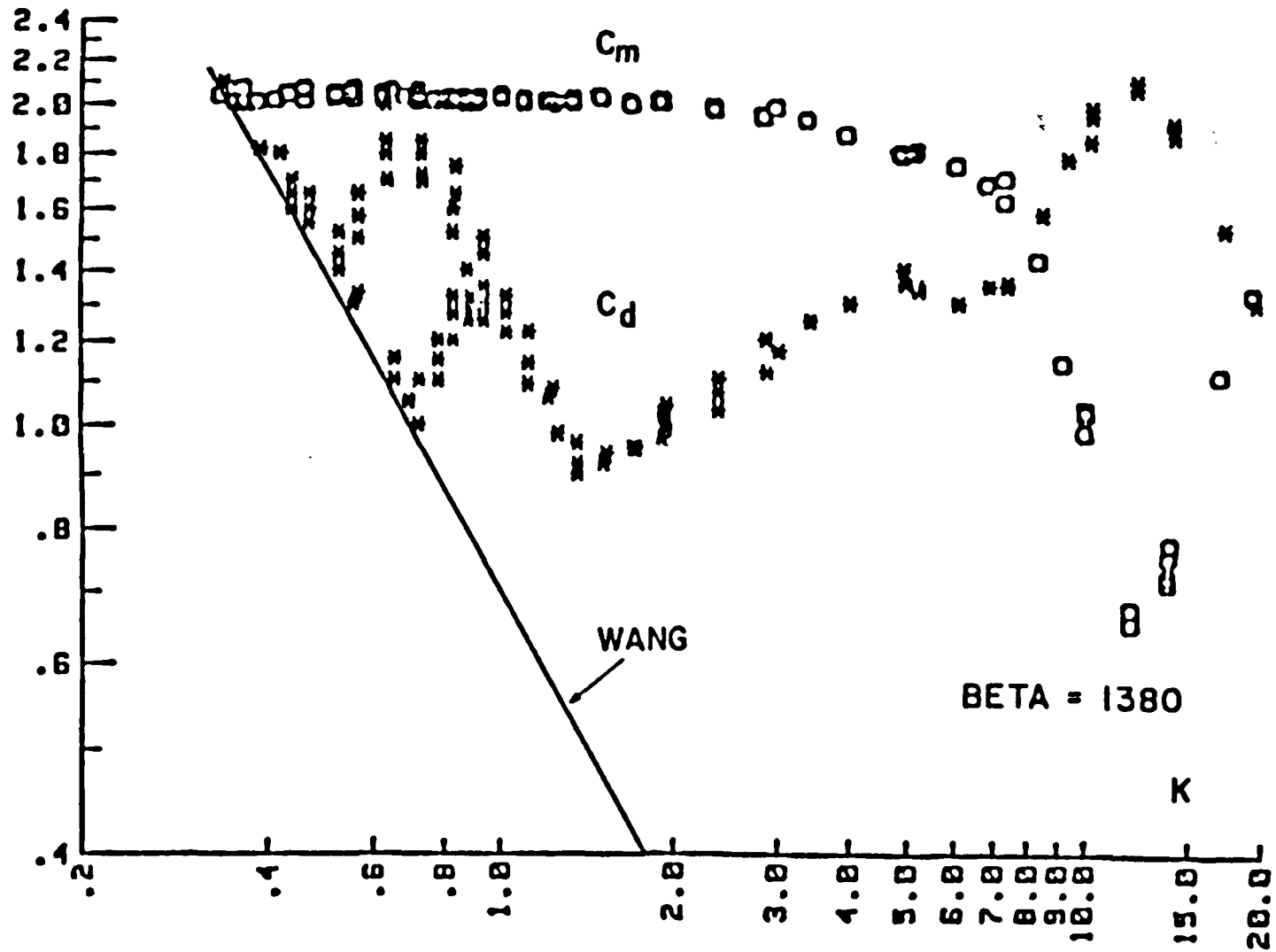

Figure 5. Drag and Inertia Coefficients versus K for β = 1380, Smooth Cylinder

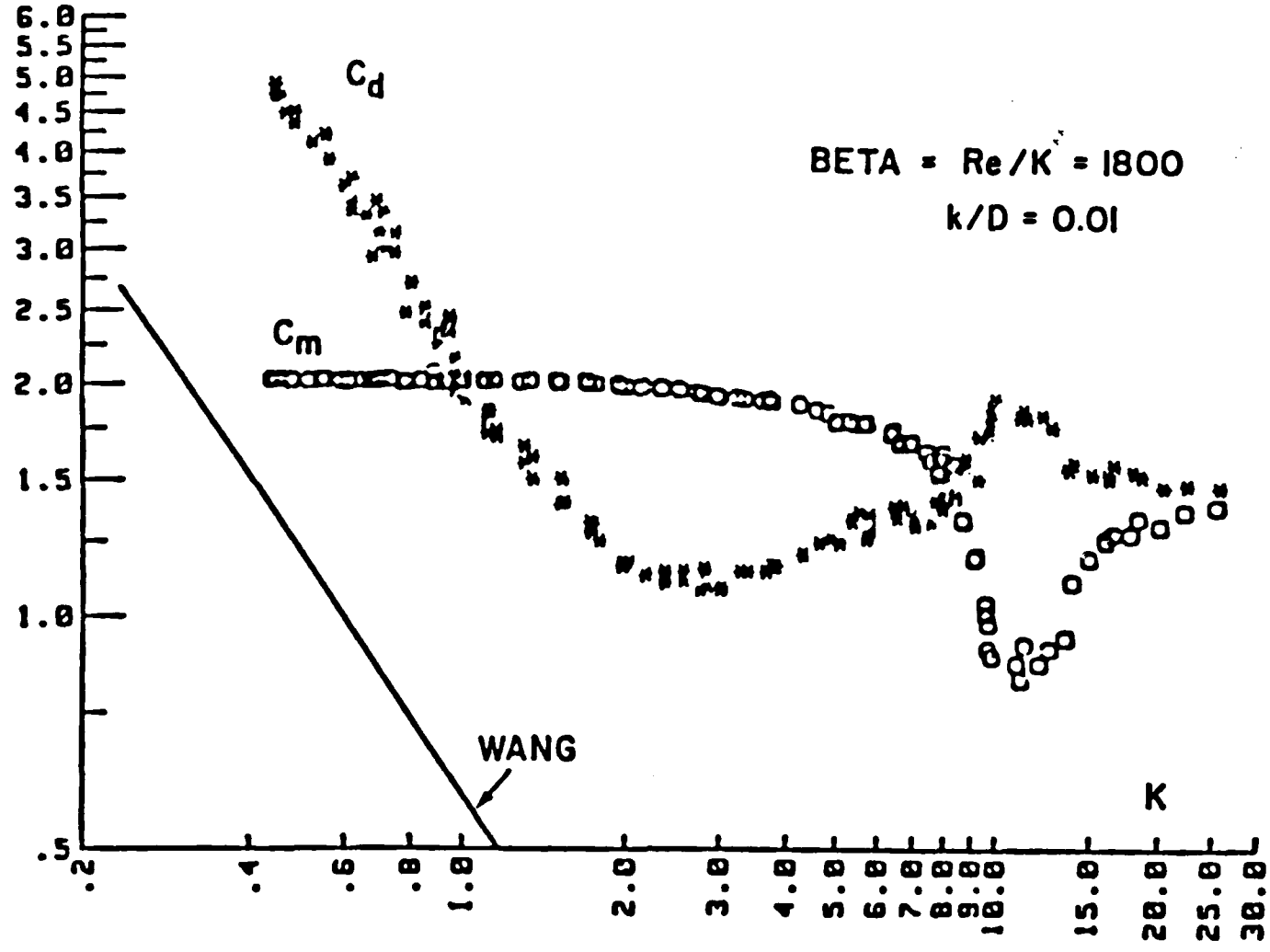

Figure 6. Drag and Inertia Coefficients versus K for β = 1800, Rough Cylinder

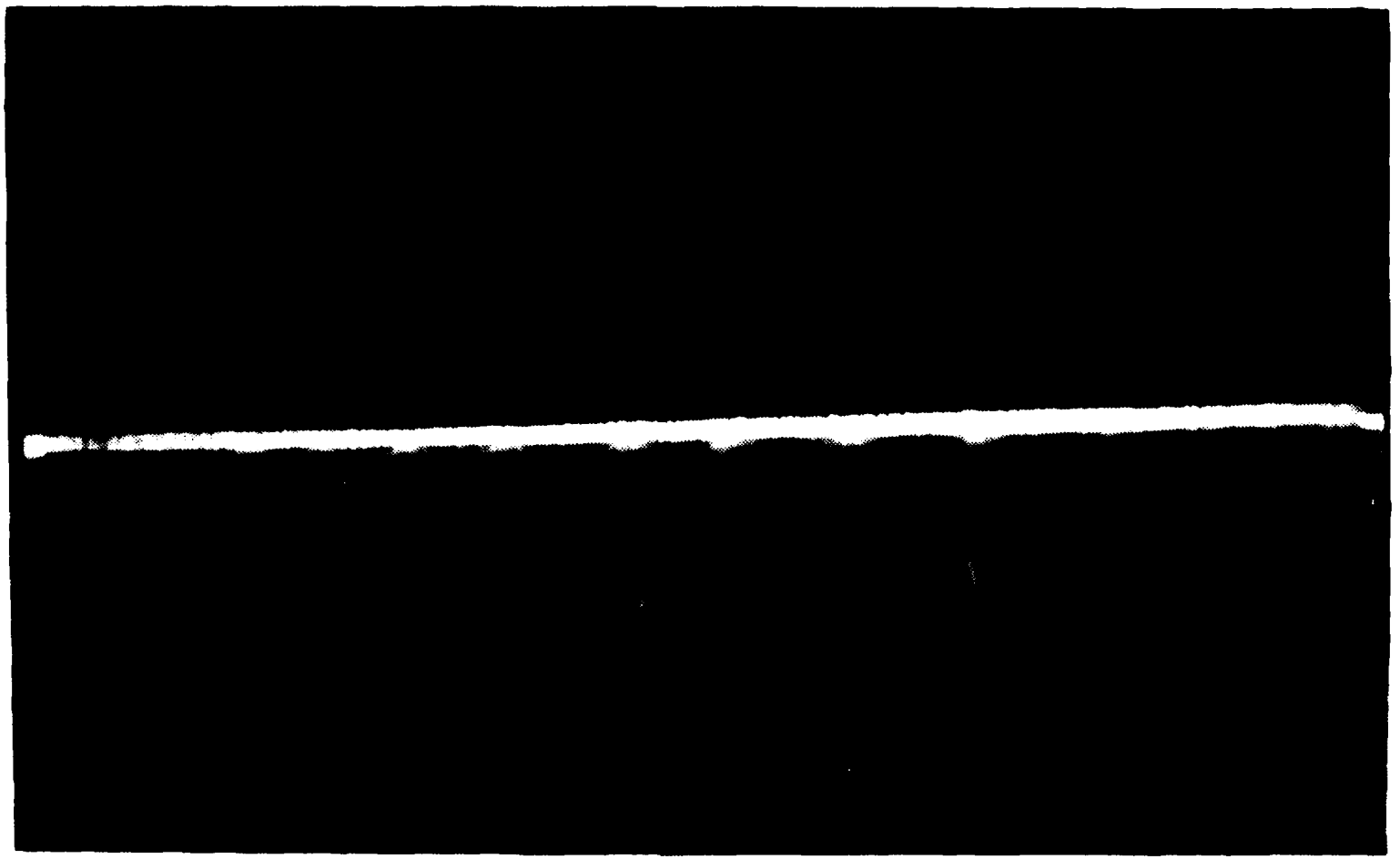

Figure 8. Photograph of Flow Visualization with a Smooth Cylinder

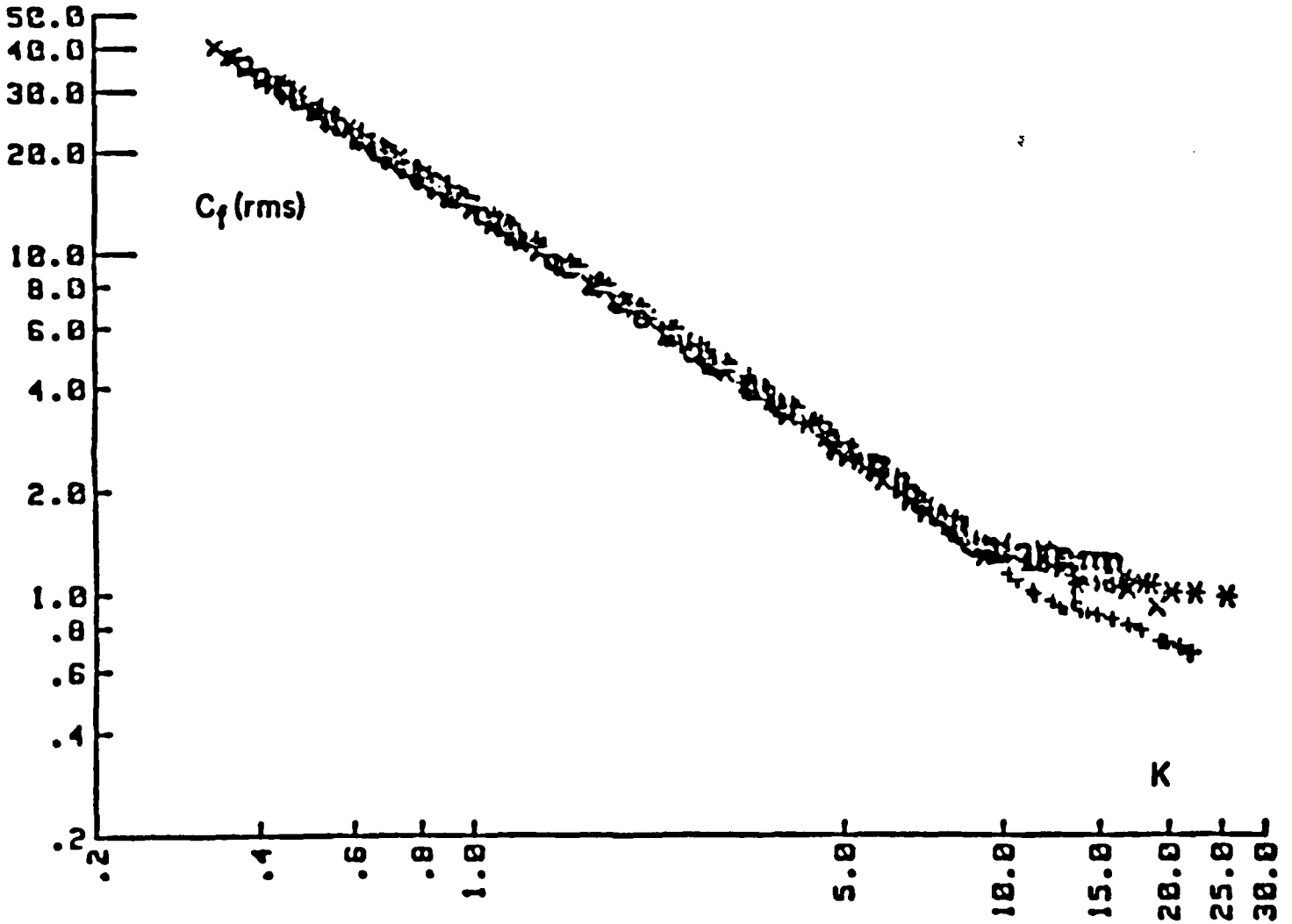

Figure 7. C_f(rms) versus K for β = 1035, β = 1380, β = 1800

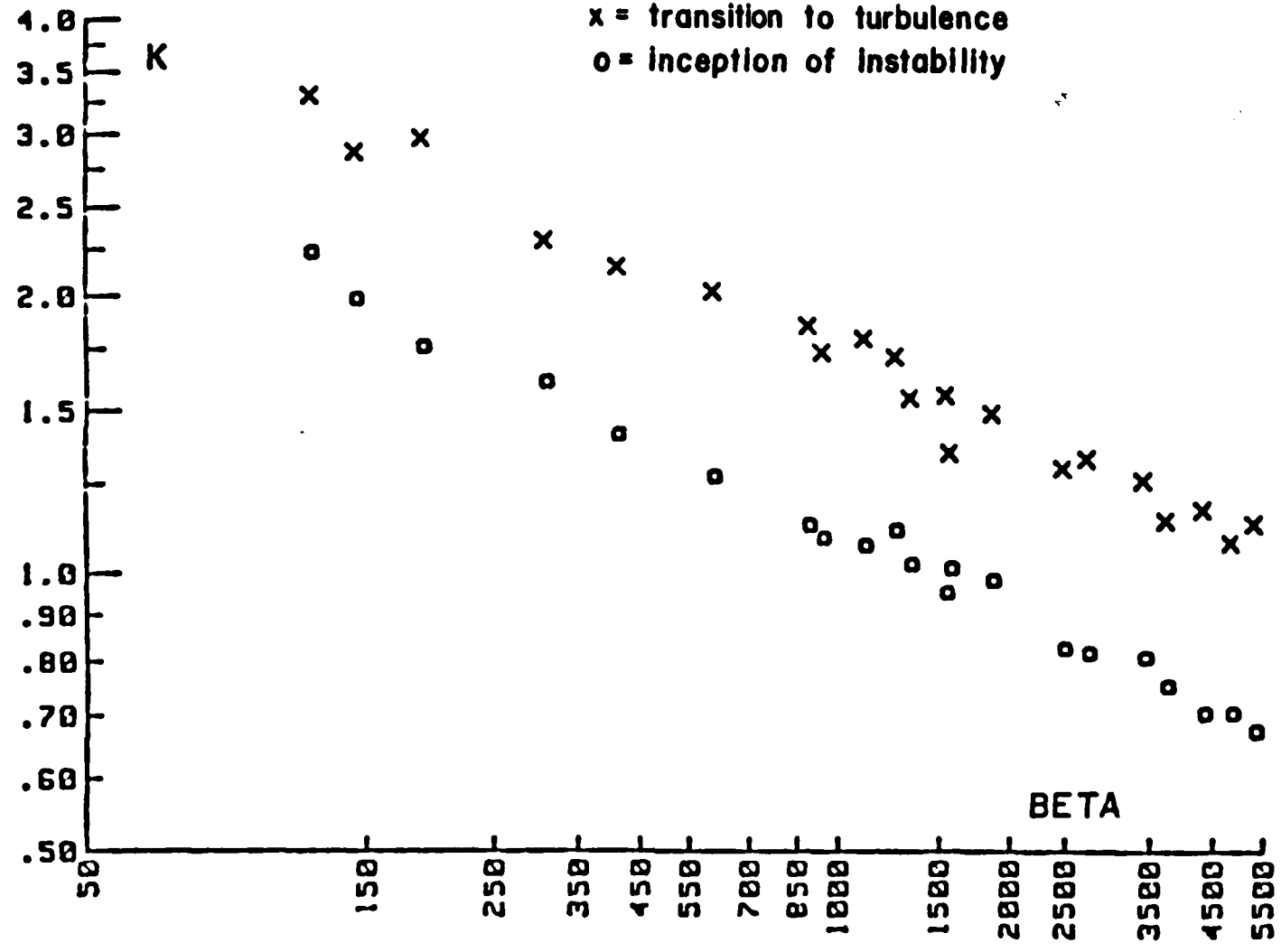

Figure 9. Critical Values of K versus β for Smooth Cylinder

LIST OF REFERENCES

1. Sarpkaya, R. and Isaacson, M., Mechanics of Wave Forces On Offshore Structures, Van Nostrand Reinhold, New York, 1981.

2. Morison, J. R., O'Brien, M. D., Johnson, J. W., and Schaff, S. A., "The Forces Exerted by Surface Waves on Piles," Petroleum Transactions AIME, v. 189, 1950.

3. Schlichting, H., Boundary-Layer Theory, McGraw-Hill Company, New York, Seventh Edition, 1979.

4. Schlichting, H., "Berechnung ebener periodischer Grenzschichtstromungen," Physikalische Zeit, v. 33, pp. 327-335, 1932.

5. Stokes, G. G., "On the Effect of the Internal Friction of Fluids on the Motion of Pendulums," Cambridge Philosophical Transactions, IX, pt. 2, pp. 8-106, 1851.

6. Rosenhead, L. (Ed.), Laminar Boundary Layer, Osford Univ. Press, Oxford, 1963.

7. Wang, C. Y., "On High-Frequency Oscillatory Viscous Flows," J. Fluid Mech., v. 32, pt. 1, pp. 55-68, 1968.

8. National Bureau of Standards Report No. 4821, Forces on Cylinders and Plates in the Oscillating Fluid, by G. H. Keulegan and L. H. Carpenter, 1956.

9. Rajabi, F., Hydroelastic Oscillations of Smooth and Rough Cylinders in Harmonic Flow, Ph.D. Thesis, Naval Postgraduate School, Monterey, California, 1980.

10. Bakmis, C., Harmonic Flow about Cylinders, M.E. Thesis, Naval Postgraduate School, Monterey, California, 1980.

11. Taneda, S., Honji, H., and Tatsuno, M., "The Electrolytic Precipitation Method of Flow Visualization," Proceedings of theh International Symposium on Flow Visualization, Edited by Asanuma, T., October 1977.

INITIAL DISTRIBUTION LIST

		No. Copies
1.	Defense Technical Information Center Cameron Station Alexandria, Virginia 22304-6145	2
2.	Library, Code 0142 Naval Postgraduate School Monterey, California 93943-5100	2
3.	Professor T. Sarpkaya, Code 69Sl Mechanical Engineering Naval Postgraduate School Monterey, California 93943-5100	5
5.	Chairman Department of Mechanical Engineering, Code 69 Naval Postgraduate School Monterey, California 93943-5100	2
6.	LT Nathan Q.S. Yuen, USN 2015 Kilakila Drive Honolulu, Hawaii 96817	2

END

FILMED

12-85

DTIC